

Laser absorption and ion acceleration under tight-focusing conditions

O. Klímo^{1,2}, P. Valenta^{1,2}, S. Weber²

¹ FNSPE, Czech Technical University in Prague, 11519 Prague, Czech Republic

² Institute of Physics of the ASCR, ELI-Beamlines, 18221 Prague, Czech Republic

Focusing of an intense laser beam to tight sub- μm spot can be achieved using a curved plasma mirror [1]. An order of magnitude increase in focused intensity can be achieved in comparison with a typical f/3 off-axis parabolic mirror. Not only the higher intensity, but also the strong radial ponderomotive force and longitudinal electric field component affect the trajectories of electrons in the focal spot region modifying the absorption process and consequently also ion acceleration. These processes are investigated here in 2D geometry using kinetic simulations for an intense laser pulse with the waist w_0 in the range 0.6-5 λ (λ is the laser wavelength).

We start with theoretical analysis of the influence of the longitudinal electric field component. In the following, we assume a Gaussian profile in the focal spot so that the transverse field of the linearly polarized laser wave can be described as

$$E_y(x, y) = E_{y0} \sin(kx) \exp\left(-\frac{y^2}{w_0^2}\right), \quad (1)$$

where $k = 2\pi/\lambda$, E_{y0} is the electric field amplitude given by $E_{y0} = \sqrt{2I/c\epsilon_0}$, c is the speed of light and ϵ_0 is the vacuum permittivity. We also assume that the laser pulse is relatively long and we neglect the dependence of its amplitude on the longitudinal coordinate x . The longitudinal electric field amplitude E_{x0} is maximum at $y = w_0/\sqrt{2}$, where the gradient of E_y reaches its extremum. This amplitude results from the Poisson equation (in vacuum) as

$$E_{x0} = \frac{E_{y0}}{kw_0} \sqrt{\frac{2}{e}}, \quad (2)$$

where e is the Euler's constant. The ratio between the transverse and the longitudinal field amplitude is thus about $7.3 \times w_0/\lambda$, i.e. the transverse field is by far dominant even for a diffraction limited Gaussian beam.

However, the longitudinal field may still influence the absorption process as the transverse field by itself is not responsible for hot electron generation. This is the case especially if the focal spot size is so small that the transverse electron oscillation in the laser field is comparable or smaller than $w_0/\sqrt{2}$. In this case, an electron can get from the centre of the focal spot to the place of a strong longitudinal field in a half laser period and his trajectory may thus be significantly influenced. Assuming that the transverse speed of electron in a strong laser wave

is close to the speed of light, one may estimate that this happens when $w_0/\sqrt{2} \leq \lambda/2$. For the laser wavelength of 800 nm, this gives $w_0 < 0.6 \mu\text{m}$.

The kinetic simulations of laser-plasma interaction and particle acceleration are performed using PIC code EPOCH [2] in 2D geometry. The tight focusing is implemented using the approach [3], which allows to pre-calculate the electromagnetic field distribution at the boundary of the simulation box at each time step even for focal spot sizes, where the paraxial approximation is not applicable. A fully ionized hydrogen target with the density of $100 \times$ the critical density and the thickness of $2 \mu\text{m}$ is irradiated by a linearly polarized 30 fs long and tightly focused laser beam at normal incidence. The laser wavelength is $\lambda = 800 \text{ nm}$ and the peak intensity is varied in the range $I = 10^{20} - 10^{22} \text{ W/cm}^2$. The same intensity is always used for different waists to investigate only the influence of the spot size. However, one must take into account that the total laser pulse energy scales with w_0 in our 2D simulations and thus the results are normalized to the laser pulse energy.

The laser energy absorption versus the waist of the beam is plotted in Fig. 1 for different laser intensities. Apart from the fact that the laser energy absorption increases with laser intensity there is a significant increase in absorption also for very tight focusing. This increase is observed for all three intensities and similar waist size and it is consistent with our theoretical estimate.

The energy distributions of all electrons in the simulation box normalized to the laser energy are plotted in Fig. 2 at the time, when the peak laser intensity interacts with the target (will be referred to as t_0 in the following). The distributions of electrons for $w_0 \gtrsim 1 \mu\text{m}$ do not show significant difference for the laser pulse intensities 10^{20} and 10^{21} W/cm^2 . A significant increase in the number of hot electrons and their cut off energy is observed for very tight focusing with $w_0 = 0.5 \mu\text{m}$. The case of the highest intensity 10^{22} W/cm^2 is different because of significant hole boring. The laser field is self-focused for the case of the largest spot size. As a result of this process the laser pulse intensity is about 2 times higher for $w_0 = 4 \mu\text{m}$ than for $w_0 = 0.5 \mu\text{m}$ and the cut off energy of hot electrons is higher too. On the other hand, the number of hot electrons in the energy range 10-50 MeV per laser pulse energy is significantly higher for the smallest spot size.

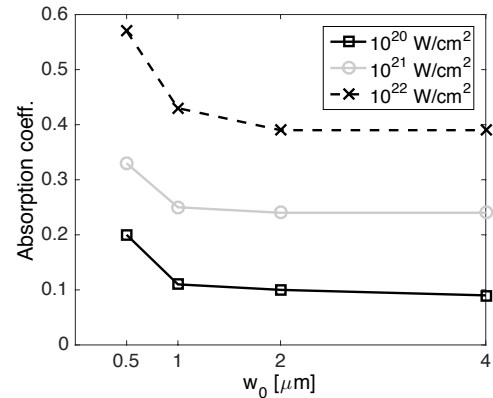


Figure 1: *Laser energy absorption in a dense hydrogen target for different laser intensities and waists of the Gaussian laser beam in the focal spot.*

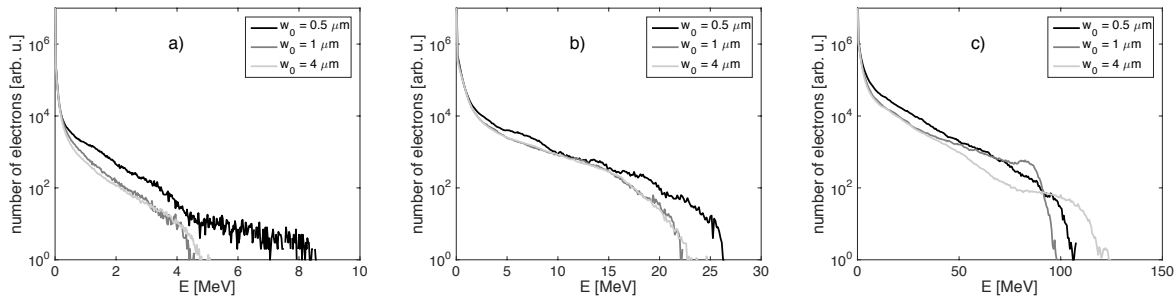


Figure 2: Energy spectra of electrons in the whole simulation box at the time of the interaction with the peak laser intensity (referred to as t_0 in the following). The intensity is a) $I = 10^{20} \text{ W/cm}^2$, b) $I = 10^{21} \text{ W/cm}^2$, c) $I = 10^{22} \text{ W/cm}^2$. The number of electrons on the vertical axis is normalized to the laser energy, i.e. divided by w_0 .

The spatial distribution of the average kinetic energy of electrons is shown in Fig. 3 a) at $t = t_0 - 20 \text{ fs}$. The laser pulse is propagating from the left to the right along $y = 0$. Two white lines are included in this figure to guide the eye. They show the divergence angle of the laser beam. It can be seen that this angle restricts the propagation of hot electron in the backward direction (with respect to laser propagation) from the target surface. The reason for this restriction is the ponderomotive force of the laser beam which pushes electrons from the high intensity region.

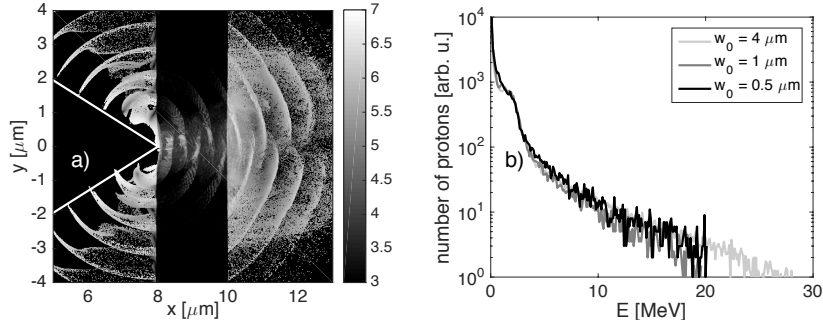


Figure 3: a) Spatial distribution of the average kinetic energy of electrons in eV (grey scale is in log units) about 20 fs before the peak laser intensity arrives to the target. b) Energy distribution of protons accelerated in the forward direction for the laser pulse intensity 10^{21} W/cm^2 about 120 fs after the end of interaction.

The bunches of hot electrons accelerated at the front target surface are separated by one laser wavelength and phase shifted by half wavelength comparing the top and the bottom side. This is the result of the strong longitudinal component of the laser field. The transverse laser field E_y ejects electrons from the focal spot in each laser cycle along the y axis in the positive and negative direction and as these electrons get into the region of strong longitudinal field, they are accelerated either forwards into the target or backwards. The final direction of electron acceleration depends on the phase of the field.

The phase shift of the bunches is explained by the opposite phase of the longitudinal field on both sides of the focal spot. The short bunches of high energy electrons are similar to the ones observed in the context of laser interaction with microscopic spherical targets in [4], where they are explained by the Mie theory. Such theory is not applicable in our case as the surface of the target is flat and the emission of bunches starts well before the surface becomes curved due to hole boring. The bunches are not so clearly observed in the later time ($t \gtrsim t_0$) because of hot electron refluxing. When the focusing is not so tight $w_0 \gtrsim 1 \mu\text{m}$, the bunches are accelerated two times per laser period and only in the forward direction as expected for the $\mathbf{v} \times \mathbf{B}$ heating [5].

The energy distributions of protons accelerated in the forward direction from the target due to the TNSA process [6] are plotted in Fig. 3 b) at $t = t_0 + 150 \text{ fs}$ for the peak laser intensity $I = 10^{21} \text{ W/cm}^2$. The distributions are again normalized per laser energy (i.e. divided by w_0). The difference between the distributions for the two tightly focused beams is relatively small. The case of $w_0 = 0.5 \mu\text{m}$ is slightly more efficient because of higher absorption. On the other hand, the angular distribution of hot electrons is wider for tight focusing and the source is so small that the hot electron cloud spread rapidly in the transverse direction and the sheath quasistatic electric field decreases. Therefore, ion acceleration due to the TNSA process is less efficient than in the case of a large focal spot size where the spreading of hot electron cloud takes much longer time. This explains the higher cut off energy of protons for $w_0 = 4 \mu\text{m}$.

In this paper, we demonstrate the influence of the beam waist of a very tightly focused intense laser beam on laser absorption, hot electron generation and ion acceleration. The qualitative change of the absorption process is observed for spot sizes with $w_0 < \lambda/\sqrt{2}$, which is supported by simple theoretical estimate and explained by the influence of the strong longitudinal electric field. This field is responsible for generation of short attosecond bunches both in the forward and backward direction. Tight focusing increases laser absorption, but it does not improve ion acceleration in the TNSA due to fast transverse spreading of electrons.

Acknowledgments: This work is supported by Czech Science Foundation project 15-02964S and by ELI: Extreme Light Infrastructure - phase 2 (CZ.02.1.01/0.0/0.0/15_008/0000162) from European Regional Development Fund.

References

- [1] M. Nakatsutsumi, A. Kon, S. Buffe, *et al.*, Opt. Lett. **35**, 2314–2316 (2010)
- [2] T. D. Arber, K. Bennett, C. S. Brady *et al.*, Plasma Phys. Control. Fusion **57**, 1–26 (2015)
- [3] I. Thiele, S. Skupin and R. Nuter, J. Comput. Phys. **321**, 1110–1119 (2016)
- [4] T. V. Liseykina, S. Pirner, and D. Bauer, Phys. Rev. Lett. **104**, 095002 (2010)
- [5] S. C. Wilks, W. L. Kruer, M. Tabak *et al.*, Phys. Rev. Lett. **69**, 1383–1386 (1992)
- [6] S. C. Wilks, A. B. Langdon, T. E. Cowan *et al.*, Phys. Plasmas **8**, 542 (2001)